

## Chapter 7. Injection and Extraction

### 7.1. Injection

A. Drozhdin, J. Holms, J. Lackey, C. Prior

#### 7.1.1. Introduction

Injection Painting is required to realize uniform density distributions of the beam in the transverse plane for space charge effect reduction. Painting preserves emittance at injection. The system for injection painting is located at the end of the 75.4-meter long straight section of the machine. The Proton Driver beta functions and dispersion along the injection section are shown in Fig. 7.1. Table 7.1 lists the Proton Driver parameters that are relevant the painting system design.

**Table 7.1.** Proton Driver Parameters

Kinetic energy at injection	0.6 GeV
Injected beam normalized transverse emittance (95%)	$3 \pi$ mm-mrad
Normalized transverse emittance after painting (100%)	$40 \pi$ mm-mrad
Injected beam longitudinal emittance (95%)	0.1 eV-s
Circulating beam longitudinal emittance (95%)	0.2 eV-s
Injection painting duration	90 $\mu$ s (45 turns )
Protons per bunch at injection	$3 \times 10^{11}$
Total intensity at injection	$2.5 \times 10^{13}$
RF frequency at injection	42.08 MHz
Revolution time at injection	1.996 $\mu$ s
Harmonic number	84
Number of bunches	84
Full aperture ( $2 \cdot A_x \times 2 \cdot A_y$ )	152.4 mm $\times$ 101.6 mm
Horizontal betatron tune	11.415
Vertical betatron tune	7.303
Horizontal $\beta$ at the foil	9.890 m
Horizontal $\alpha$ at the foil	-3.243
Horizontal dispersion at the foil	0.0 m
Vertical $\beta$ at the foil	12.534 m
Vertical $\alpha$ at the foil	3.833
Horizontal beam size at injection in the foil	$\sigma_x = 1.95$ mm
Vertical beam size at injection in the foil	$\sigma_y = 2.20$ mm
Horizontal position of injected beam at the foil	27.00 mm
Horizontal angle of injected beam at the foil	9.529 mrad
Horizontal beam half-size at injection after painting	17.45 mm
Vertical beam half-size at injection after painting	19.64 mm

### 7.1.2. Injection Painting Scheme

Injection painting is performed by using two sets of fast horizontal and vertical magnets (kickers). The proton orbit is moved in the horizontal plane at the beginning of injection by 24.7 mm to the thin graphite stripping foil to accept the first portion of protons generated by  $H^-$  in the foil (Fig. 7.2). Three 1-m long kicker magnets are used to produce the orbit displacement (Fig.7.3). The maximum field of the kicker magnets is 0.19 kG. The horizontal kick at the beginning of injection is shown in Fig. 7.3. Gradual reduction of kicker strength permits "painting" the injected beam across the accelerator aperture with the required emittance. Vertical kicker magnets located in the injection line (not shown) provide injected beam angle sweeping during injection time, starting from maximum at the beginning of injection and going to zero at the end of painting process. Horizontal and vertical kickers produce abetatron amplitude variation during injection. This results in a uniform distribution of the circulating beam after painting. Painting starts from the central region of phase space in the horizontal plane and from the border of it in the vertical plane, and goes to the border of the beam in the horizontal plane and to the center in the vertical plane. This produces a so-called "uncorrelated beam" with elliptical cross section, thereby eliminating particles that have maximum amplitudes in both planes simultaneously.

A septum-magnet located upstream of the foil (Fig. 7.3) is used to separate the proton and  $H^-$  beams at the quadrupole upstream of the foil by 400 mm. This allows the  $H^-$  beam to pass outside the quadrupole body. The beam dump located behind the stripping foil is used for  $H^0$  interception. Injection kickers cause negligible perturbation of the  $\beta$  functions and dispersion at injection. Horizontal dispersion in the foil at injection is equal to -0.027 m.

Multi-turn particle tracking through the accelerator is done with the STRUCT [2] code. A stripping foil made of  $300 \mu\text{g}/\text{cm}^2$  ( $1.5 \mu\text{m}$ ) thick graphite has the shape of a so-called corner foil, where two edges of the square foil are supported and the other two edges are free. The foil size is  $1.6 \text{ cm} \times 3.0 \text{ cm}$ .

The time dependence of kicker magnet strength is chosen to obtain uniform distribution of the beam after painting in both the horizontal and vertical planes. Eqs. 7.1 and 7.2 (horizontal) and Eq. 7.3 (vertical) are the equations for the optimal bump-magnet wave forms [3] as simulated in the STRUCT code.  $N$  is the turn number from the beginning of painting.

$$B = B_0 \left[ 0.5815 + 0.4185 \left( 1 - \sqrt{\frac{2N}{45} - \left(\frac{N}{45}\right)^2} \right) \right] \quad N < 45 \quad (7.1)$$

$$B = B_0 \left[ 0.5815 - \frac{N - 45}{10.31.85} \right] \quad N > 45 \quad (7.2)$$

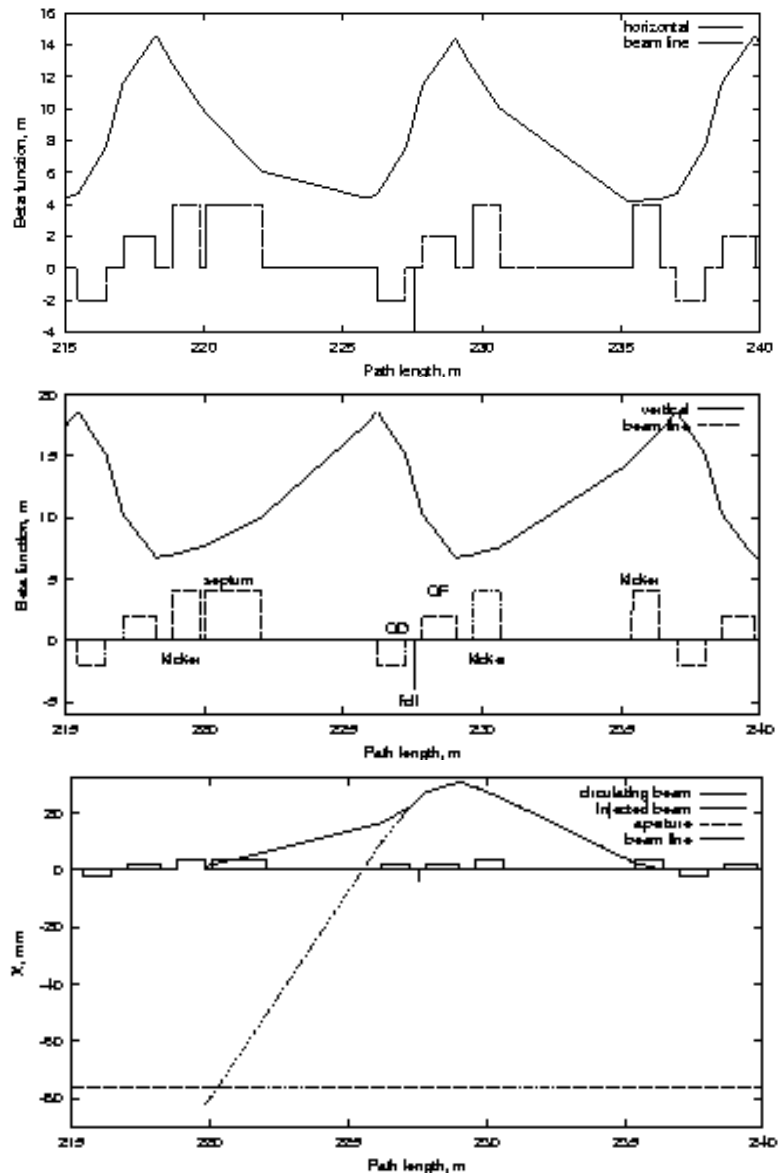


**Figure 7.1.** Horizontal (top), vertical (middle) beta functions, and painting bump (bottom) at injection.

$$Y' = Y'_0 \sqrt{2 \frac{45 - N}{45} - \left( \frac{45 - N}{45} \right)^2} \quad Y'_0 = 1.0395 \text{ mrad} \quad (7.3)$$

The horizontal and vertical phase planes of the injected beam in the foil are shown in Fig. 7.4. The emittance of the injected beam at 95% is equal to  $3 \pi$  mm-mrad.

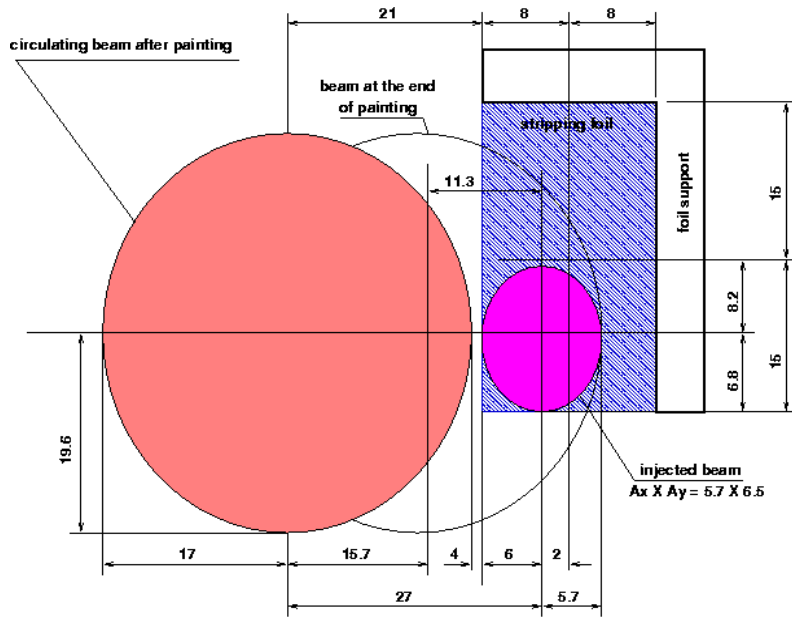


**Figure 7.2.** Injected and circulating beam locations in the foil at painting.

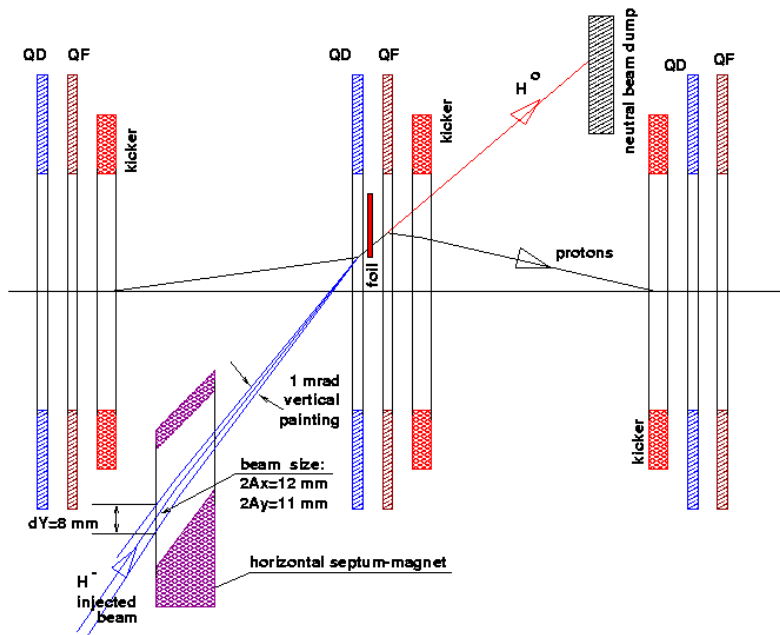


**Figure 7.3.** Injection painting scheme.

Painting lasts during 45 turns, and after painting the circulating beam moves out of the foil during 6 turns. In the simulations the horizontal bump amplitude at the foil is 27 mm = 11.3 mm (painting) + 15.7 mm (removing from the foil) (Fig. 7.2). Vertical angle variation is 1.0395 mrad. The horizontal and vertical phase planes of the circulating beam in the foil at 6<sup>th</sup>, 45<sup>th</sup>, and 51<sup>st</sup> turns from the beginning of painting are presented in Fig. 7.5.

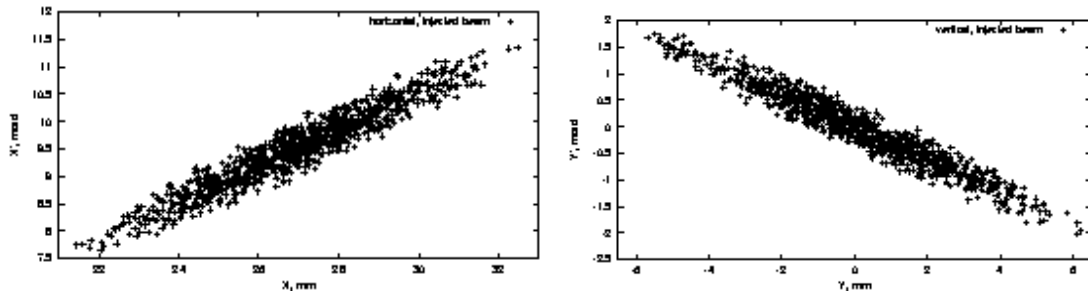


**Figure 7.4.** Horizontal (left) and vertical (right) phase plane of injected beam at the foil.

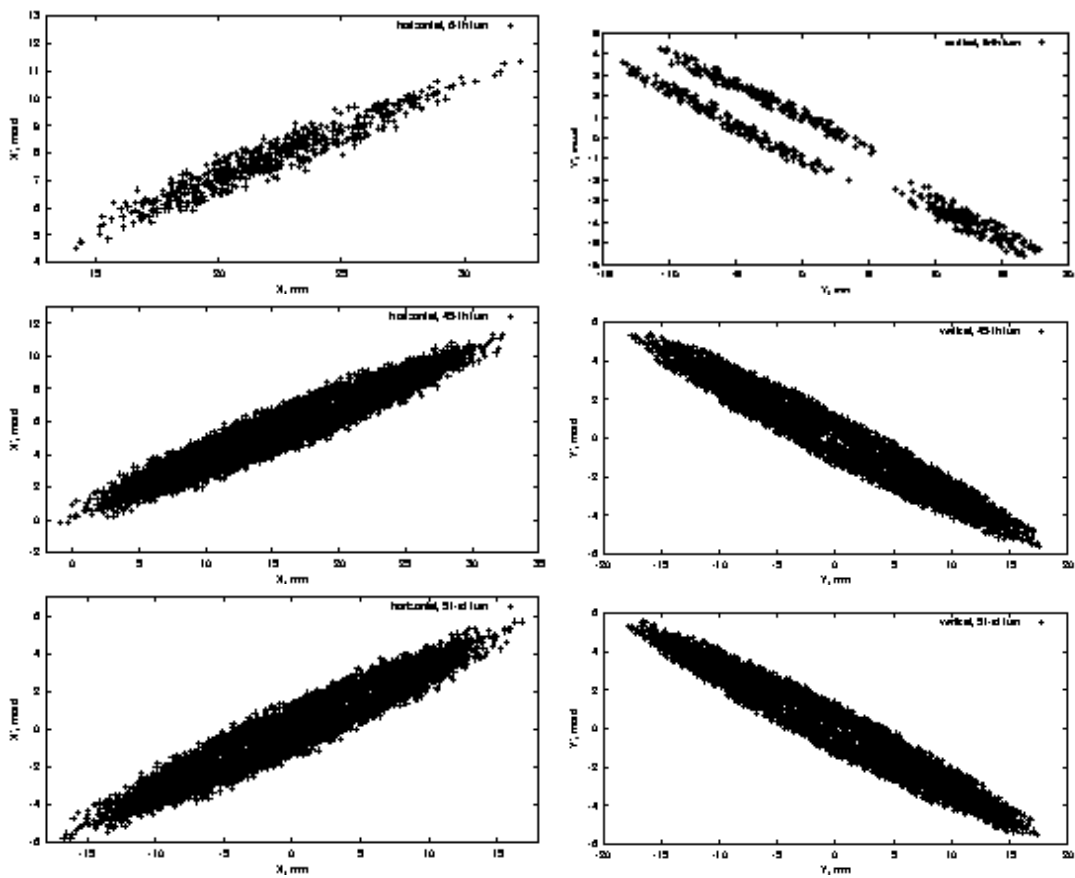


**Figure 7.5.** Horizontal (left) and vertical (right) phase plane in the foil at 6<sup>th</sup> (top), 45<sup>th</sup> (middle), and 51<sup>st</sup> (bottom) turn from the beginning of beam painting.

The horizontal kicker magnet strength and the vertical angle of the beam in the foil during injection are presented in the top part of Fig. 7.6. Particle transverse population and particle density distribution after painting at the foil location are shown in the middle and at the bottom of Fig. 7.6. Circulating beam after painting (51<sup>st</sup> turn) and particle population at the foil are shown in Fig. 7.7. Particle distribution at the foil is shown in Fig. 7.8.

The average number of hits upon the stripping foil for each particle is 5.22. This effects low-level nuclear interactions and multiple Coulomb scattering in the foil at injection, and because of this causes low-level particle loss at injection.

The circulating protons pass several times through the foil and some of them can be lost because of scattering in the foil. Multiple Coulomb scattering is very small because of small foil thickness. Particle energy loss in the foil at one pass is  $1.6 \times 10^{-6}$  of the initial energy. The total rate of nuclear interactions in the foil during the process is  $2.0 \times 10^{-5}$  of the injected intensity. The emittance of the circulating beam in the horizontal plane is small in the beginning of painting and it gradually reaches maximum at the end of painting. Therefore the particle horizontal amplitude, on average, is sufficiently smaller than the accelerator aperture. Particles can be lost only during the first few turns after injection, and only in the region of injection kick maximum where the beam is close to the accelerator aperture. At every subsequent turn after particles are injected, they move away from the aperture restriction because of the fast reduction in the painting kick amplitude. Simulations have shown that the rate of particle loss in the accelerator from interaction with foil is as low as  $7.3 \times 10^{-5}$  of the injected intensity.

The calculated stripping efficiency is 99.2% and the estimated yield of excited states  $H^0(n)$  atoms with  $n \geq 5$  is equal to 0.016% [4]. These atoms will be stripped into protons before they reach the dump and become a beam halo. The remaining excited atoms ( $n \leq 4$ ) have a longer lifetime and they will go to the neutral beam dump.

### 7.1.3. Septum and Kicker Magnets Parameters

Septum and kicker magnets parameters are presented in Table 7.2. The septum is curved to reduce the pole-tip width.

**Table 7.2.** Septum and Kicker Magnets Parameters

Element	Field	Current	Inductance	Length	Poletip width	Pole-tip gap	Turns number	Septa thick.
Name	Gauss	Amps	$\mu H$	m	mm	mm		mm
Septum	2135	6720	2.538	2	40	40	1	15
kicker-1	108	37.98	126	1	152	102	8	-
kicker-2	92	22.48	126	1	152	102	8	-
kicker-3	212	74.40	126	1	152	102	8	-

### 7.1.4. Stripping Foil Design

Carbon stripping with densities between 300 and 600  $\mu g/cm^2$  have been in use in the Booster since the 400 MeV Linac upgrade. No foils have ever been lost because of beam damage. It should be pointed out, however, that the Booster uses nominally 11 injection turns per cycle and the Proton Driver will use up to 45 turns per cycle.

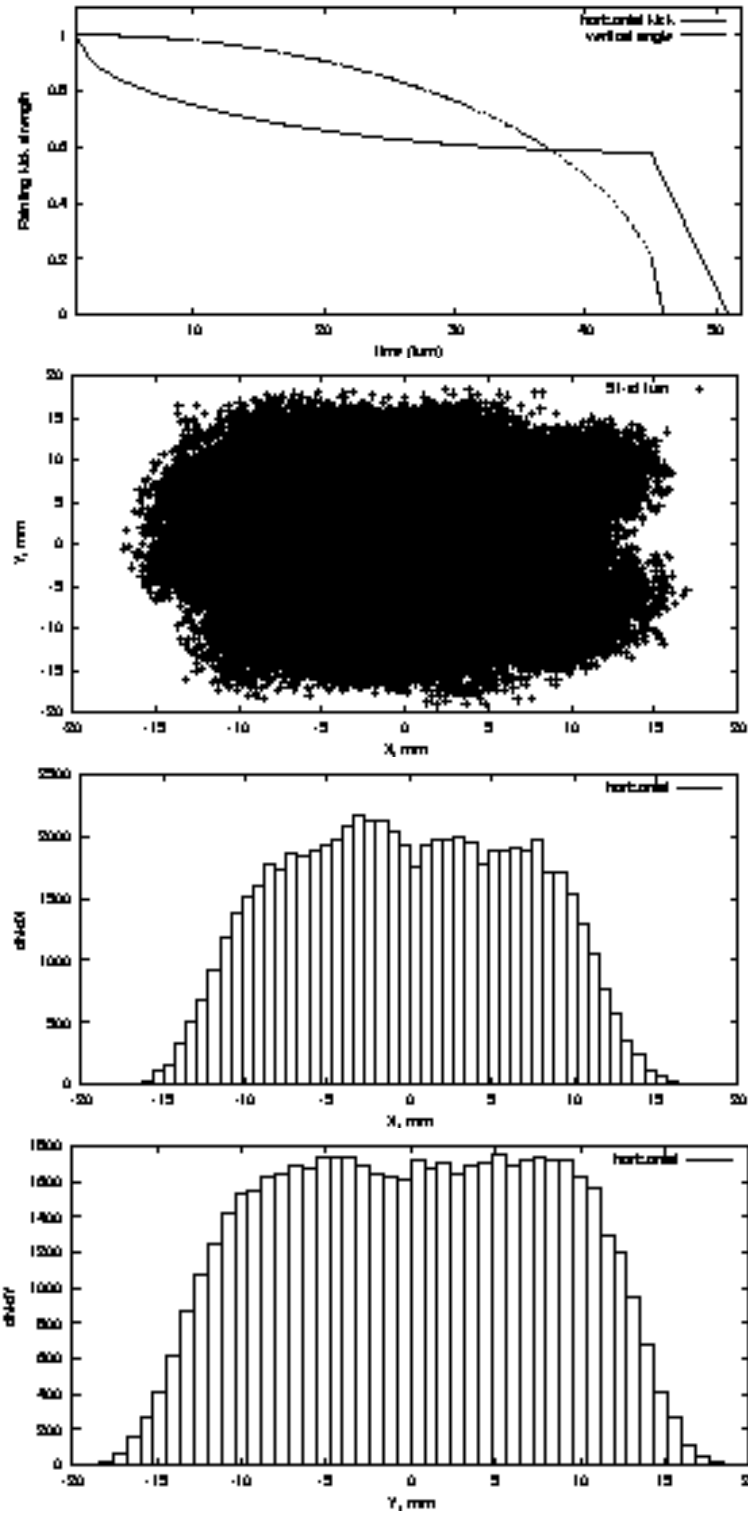


**Figure 7.6.** Horizontal kicker strength and vertical angle of the beam at injection in the foil (top). Particle transverse population (middle) and particle density distribution in the foil (bottom two figures) at 51<sup>st</sup> turn from the beginning of beam painting.

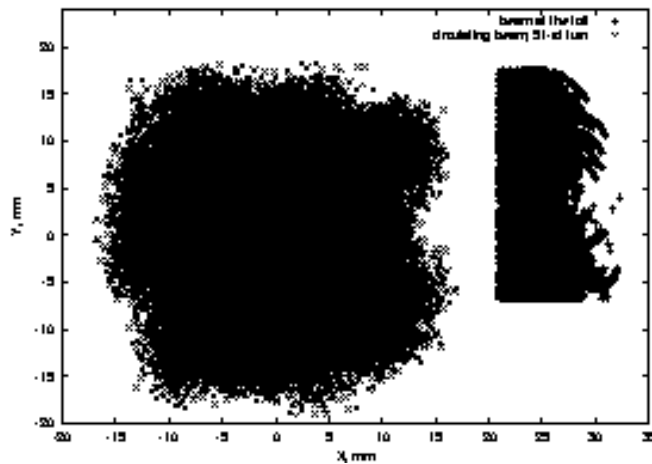


**Figure 7.7.** Circulating beam after painting (51<sup>st</sup> turn) and particle population at the foil.

The Booster also typically operates at a reduced duty factor, less than 1 Hz, whereas the Proton Driver will operate at 15 Hz continuously. The Booster operational repetition rate will change in the future with the Boone and NuMI experiments to as high as 10 Hz. It is possible that foil damage may become a factor and will have to be dealt with.

There are two basic concerns with the Proton Driver foils, heat dissipation and type of mount.

The stripping foil will reach temperatures of ~800 K. This temperature may be of concern in the mounting of the foil. The Fermilab Booster foils are simply bonded to a thin copper support with super glue. There has never been a problem with this kind of mounting. However the Booster has never run beam at 15 Hz for sustained periods, so average temperature rise has never been a problem. If the foil actually reaches sustained temperatures this high, another mounting technique may have to be used. Keep in mind that even though the foil may get very hot at the beam location, the foil is exceedingly thin and the amount of heat transmitted to the foil holder will be small. The metal holder will be capable of dissipating a large amount of heat relative to the foil so a simple glue bond may suffice. This is not considered a serious matter; however, there are many ways of mounting the foil.

The foil will have two free edges and this is also of some concern. (See Fig. 7.2 for the foil dimensions.) Carbon foils this thin have a tendency to curl up. If this proves to be the case then the foil may have to be mounted with only one free edge as done in the Booster. However this means the foil will be approximately twice as long. This is not desirable since there would be more interactions of the circulating beam with the foil. On the other hand, if necessary, it can be done.

### 7.1.5. Conclusions

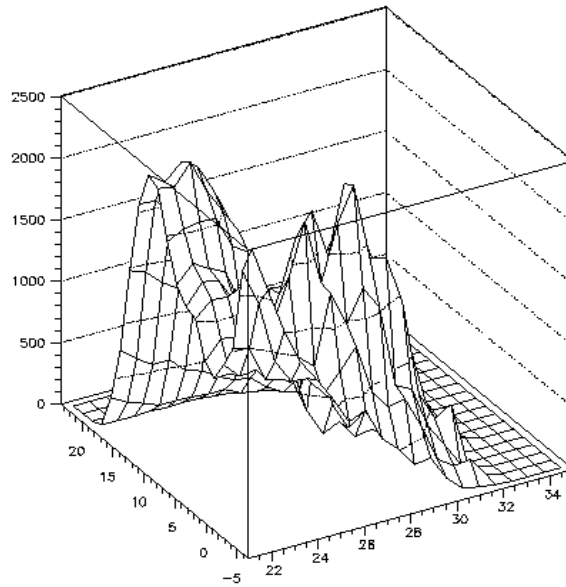
An injection painting system, consisting of two sets of horizontal and vertical kicker magnets, produces the quasi-uniform density distribution of the circulating beam required for the beam space charge effect reduction and emittance preservation at injection.

The calculated stripping efficiency is 99.2%, and the estimated yield of excited  $H^o(n)$  atoms with  $n \geq 5$  is 0.016%. These atoms will contribute protons to the beam halo.

The temperature buildup during the injection pulse and steady state temperature of the foil are calculated from an analytical distribution of proton hits using ANSYS code. The instantaneous temperature buildup, calculated with contributions of multiple collisions, ionization loss from protons and electrons accompanying the stripping process, is a little less than 200 K.

With only emission as a cooling mechanism, the foil temperature reaches a steady state of ~800 K after about 10 cycles of injection, that is in less than one second.

z2/03/29 10.46



z2/03/29 10.46

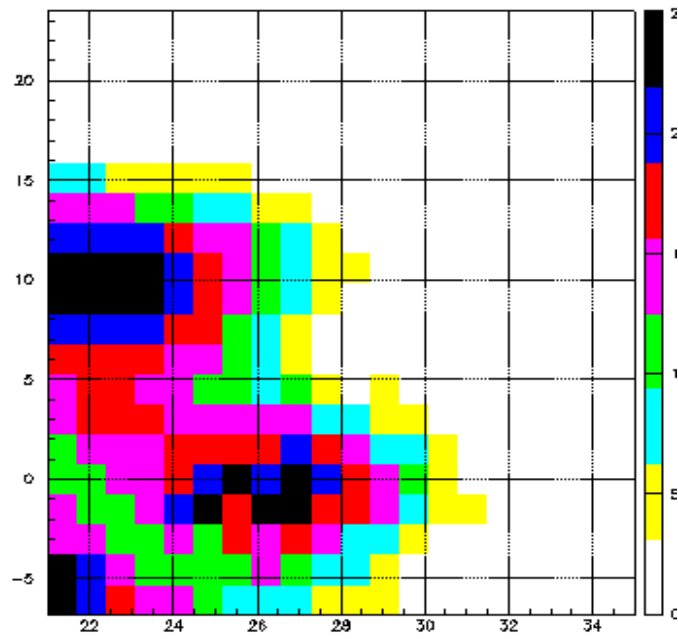


**Figure 7.8.** Particle distribution at the foil.

## **7.2 Extraction**

J. Lackey

### **7.2.1 Introduction**

The 8 GeV beam extraction is implemented using a standard single turn fast extraction system. The system presented here is the most compact system in terms of the amount of contiguous machine circumference required to accommodate the extraction equipment. Only the drift spaces of two adjacent cells are required for all of the extraction devices and the extraction system can be inserted into any two adjacent cells in either straight section. Possible other schemes discussed in section 7.2.6 would occupy more of the machine circumference but might have other beneficial properties such as faster kicker systems requiring a smaller notch in the beam or would allow the insertion of other required machine elements between the kickers and septum.

In order to avoid beam losses on the downstream extraction elements a notch or gap in the beam is required. This notch must be of a length equal to the effective rise time of the extraction kickers. It is assumed that the notch is created external to the machine.

### **7.2.2 Extraction System Elements**

The extraction system consists of three primary elements: fast kickers, septum magnet and a system of orbit bump magnets to maintain the required circulating beam aperture with respect to the septum. The layout of the extraction system is shown in Figure 7.9. The layout of the septum and bump magnets is shown schematically in Figure 7.10.

### **7.2.3 Kickers**

The kickers are a set of five 16.67-ohm transmission line type magnets. The impedance of the kickers is chosen to be equal to the impedance of three standard 50-ohm cables connected in parallel. The next usable impedance is 25 ohms but a choice of this impedance would require more kickers than can fit into the drift space of a single cell. The use of 25-ohm kickers is discussed in section 7.2.6.

The kickers are designed to kick the beam vertically. The transverse dimensions are chosen to allow for a reasonably thick walled non-metallic beam pipe presumably made of ceramic or some other appropriate material. A magnet length of one meter will allow five kicker magnets to fit comfortably in a single drift space. The strength of the kicker system is sufficient to kick a  $90\pi$  mm-mrad beam across a 10 mm septum. The kicker parameters are listed in Table 7.3.

### **7.2.4 Septum**

In this design report the use of a single septum magnet is assumed. The aperture of the septum is designed to be as large as is reasonably possible. The larger aperture is highly desirable since it reduces alignment tolerances and allows the extraction channel to accommodate some amount of halo in the beam. The septum parameters are listed in Table 7.3.

### 7.2.5 Orbit Bumps

A set of magnets designed to create a local orbit bump in the same drift space as the septum is required to maintain a desired circulating beam aperture with respect to the septum. Maintaining a large circulating beam aperture is necessary to insure that the collimators will intercept beam losses and the extraction elements will not become radioactive. These bump magnets are necessarily very short and very strong. Their design and implementation will have to be done carefully in order to avoid creating strong perturbations to the lattice because of high order field components. Two such systems are currently in use in the present Booster and their high order fields are significant, particularly the sextupole component.

The amplitude of the local bump sets the aperture with respect to the septum. At injection the bump pushes the beam a full 2 inches below the septum. The aperture is reduced as the beam energy increases but the design is such that the circulating beam aperture underneath the septum is  $90\pi$  mm-mrad at extraction.

The design is done such that the magnets can be powered DC; ramping is not necessary. Ramping the bump magnets could potentially be beneficial but the cost would likely be prohibitive. The orbit bump magnet parameters are listed in Table 7.3.

### 7.2.6 Alternative Extraction Layouts

Other layouts for the kickers are possible. It would be possible to move the 16.67 ohm kickers upstream one cell. There the phase advance is more advantageous and the kickers could be run at lower voltages or fewer kickers could be used. However any equipment placed in the cell between the kickers and septum would have to accommodate the relatively large kick displacement of the extracted beam. The advantage of this layout is that other equipment *could* be put into the intervening cell if necessary.

One could also use lower impedance 25-ohm kickers. The advantage of lower impedance kickers is that the effective field rise time of the 25-ohm kickers is significantly shorter than the 16.67 ohm kickers and would require a shorter gap in which to rise. The cost is that at least two more kickers are required (for a total of 7) and would take up more longitudinal space in the machine.

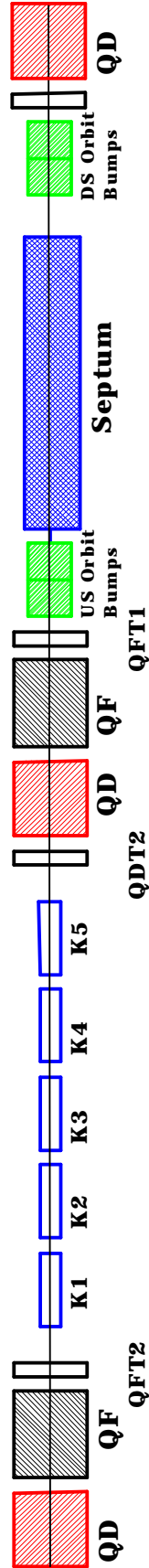


**Figure 7.9.** Vertical extraction system layout.

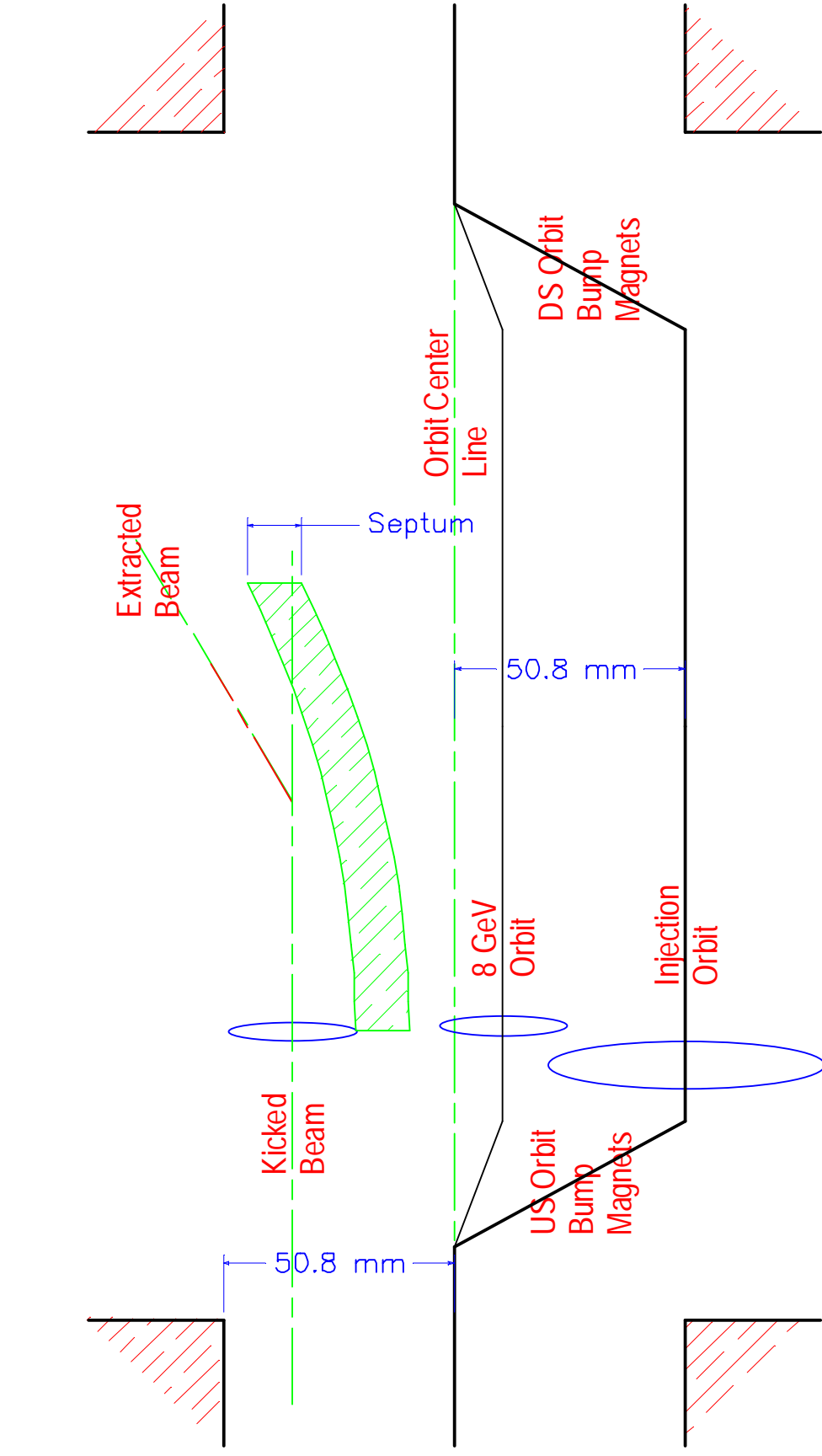


**Figure 7.10.** Orbit bump and septum in the extraction straight.

**Table 7.3.** Parameters of the Extraction System

	KICKERS	SEPTUM	ORBIT BUMPS
Number of Magnets	5	1	4
Magnet Length (m)	1	4	0.25
Insertion Length (m)	1.2	4.4	1 (2 magnets)
Effective Length (m)	1.16	4.025	0.415
Bend Center Spacing (m)	1.2	N/A	0.5
Pole tip Width (cm)	11.43	5.54	15.2
Pole tip Gap (cm)	16.51	2.54	16.51
Number of Turns	1	1	128
Inductance ( $\mu\text{H}$ )	791	10.96	7720
Nominal Current (kA)	2	21.56	0.98
Nominal Voltage (kV)	67	3	0.0202
Impedance ( $\Omega$ )	16.67	N/A	N/A
B field (Tesla)	0.0223	1.08	0.941
Bend Angle (mrad)	0.75	145.5	96.02 @ 400 MeV
Current Pulse Length ( $\mu\text{s}$ )	1.6	250	DC
Magnet Fill Time (ns)	47.5	N/A	N/A
Current Rise Time ( $\mu\text{s}$ )	0.05	125	N/A
Field Rise Time (ns)	68.9	N/A	N/A

## References

- [1] The Proton Driver Design Study, Fermilab TM-2136, December 2000.
- [2] I.S. Baishev, A.I. Drozhdin and N.V. Mokhov, STRUCT Program User's Reference Manual, SSCL-MAN-0034 (1994); <http://www-ap.fnal.gov/~drozhdin>.
- [3] JHF Accelerator Design Study Report, KEK Report 97-16, JHF-97-10, March 1998, p3-67 - 3-71.
- [4] A. Drozhdin, O. Krivosheev, "The Fermilab Proton Driver Painting Injection Simulations," FERMILAB-FN-694 (2000).